Structural Optimization 8, 168–173 © Springer-Verlag 1994

Buckling optimization of fiber-composite laminate shells considering in-plane shear nonlinearity

H.-T. Hu

Department of Civil Engineering, National Cheng Kung University, Tainan, Taiwan 70101, Republic of China

Abstract The buckling strengths of fiber-composite laminate shells with a given material system are maximized with respect to fiber orientations using a sequential linear programming method together with a simple move-limit strategy. While a modified Riks nonlinear solution algorithm is utilized to analyse the buckling and postbuckling behaviour of composite shells, both linear and nonlinear in-plane shear formulations are employed to form the finite-element constitutive matrix for fiber-composite laminae. Results of the optimization study for simply supported composite cylindrical shells using both linear and nonlinear in-plane shear formulations are presented.

1 Introduction

The use of high modulus and high strength fiber composite materials (Fig. 1) in advanced shell structures such as submarine pressure hulls, surface ships and aircraft fuselages has increased rapidly. In many situations buckling is an undesirable phenomenon in the safe and reliable design of these advanced composite shells. Since the buckling strength of fiber composite shells heavily depends on ply orientations, the proper selection of appropriate fiber orientations for a given composite material system to achieve the maximum buckling strength of composite shells becomes a crucial problem.

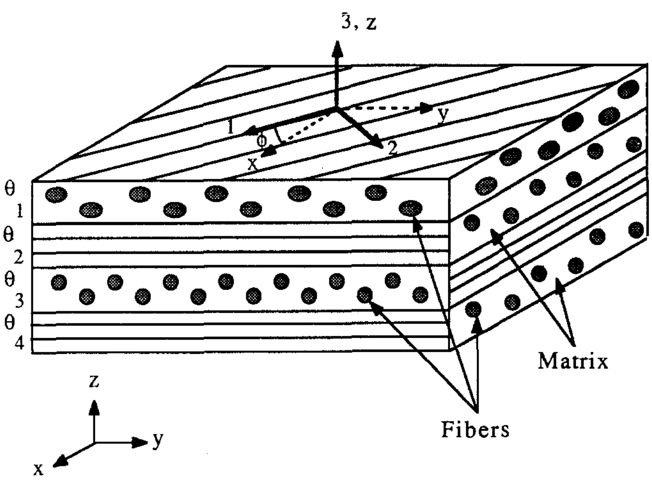

Fig. 1. Material and element coordinate systems for a fiber composite laminate

Most buckling optimization studies of composite shells have dealt with linear material properties (Sun and Hansen 1988; Hu and Wang 1992). However, the nonlinear in-plane shear is expected to have significant influence on the load bearing capacity of composite laminae (Hahn and Tsai 1973; Hashin *et al.* 1974). Hence in this study, optimization for the buckling resistance of fiber-composite laminate cylindrical shells with respect to fiber orientations including the nonlinear in-plane shear is presented. For comparison purposes, optimization using the linear in-plane shear stress-strain relation is also carried out. The buckling strengths of composite shells are computed by the finite element program ABAQUS (Hibbitt *et al.* 1993) and the optimization is done by a sequential linear programming technique together with a simple move-limit strategy (Zienkiewicz and Champbell 1973; Vanderplaats 1984)

In this paper, the nonlinear constitutive matrix for a single lamina, the constitutive matrix for a shell section, the nonlinear finite element buckling analysis, and the sequential linear programming method are briefly discussed. Then numerical results for the buckling optimization of simply supported composite cylindrical shells subjected to external hydrostatic compression with different laminate layups, $[\pm\theta/90_2/0]_S$ and $[\pm\phi/90_2/0_2/90_2/\mp\theta]$, are presented, where θ and ϕ are design variables. Finally, conclusions obtained from this study are given.

2 Constitutive matrix for single lamina

For fiber-composite laminate materials, each lamina can be considered as an orthotropic layer in a plane stress condition. If we define $\boldsymbol{\sigma}' = \{\sigma_1, \sigma_2, \tau_{12}\}^T$, $\tau_t' = \{\tau_{13}, \tau_{23}\}^T$, $\boldsymbol{\varepsilon}' = \{\varepsilon_1, \varepsilon_2, \gamma_{12}\}^T$, $\gamma_t' = \{\gamma_{13}, \gamma_{23}\}^T$, the incremental stress-strain relations for a linear orthotropic lamina in the material coordinates (Fig. 1) can be written as

$$\Delta\boldsymbol{\sigma}' = \mathbf{Q}_1' \Delta\boldsymbol{\varepsilon}', \tag{1}$$

$$\Delta\tau_t' = \mathbf{Q}_2' \Delta\gamma_t', \tag{2}$$

$$\mathbf{Q}_1' = \begin{bmatrix} \dfrac{E_{11}}{1-\nu_{12}\nu_{21}} & \dfrac{\nu_{12}E_{22}}{1-\nu_{12}\nu_{21}} & 0 \\ \dfrac{\nu_{21}E_{11}}{1-\nu_{12}\nu_{21}} & \dfrac{E_{22}}{1-\nu_{12}\nu_{21}} & 0 \\ 0 & 0 & G_{12} \end{bmatrix}, \tag{3}$$

$$\mathbf{Q}_2' = \begin{bmatrix} \alpha_1 G_{13} & 0 \\ 0 & \alpha_2 G_{23} \end{bmatrix}. \tag{4}$$

The α_1 and α_2 are shear correction factors and are taken to be 0.83.

To model the nonlinear in-plane shear behaviour, the nonlinear strain-stress relation for a composite lamina suggested by Hahn and Tsai (1973) is adopted in this study, which is given as follows:

$$\left\{\begin{array}{c}\varepsilon_1\\ \varepsilon_2\\ \gamma_{12}\end{array}\right\} = \left[\begin{array}{ccc}\dfrac{1}{E_{11}} & -\dfrac{\nu_{21}}{E_{22}} & 0\\ -\dfrac{\nu_{12}}{E_{11}} & \dfrac{1}{E_{22}} & 0\\ 0 & 0 & \dfrac{1}{G_{12}}\end{array}\right]\left\{\begin{array}{c}\sigma_1\\ \sigma_2\\ \tau_{12}\end{array}\right\} +$$

$$S_{6666}\tau_{12}^2\left\{\begin{array}{c}0\\ 0\\ \tau_{12}\end{array}\right\}. \tag{5}$$

In the above equation only one material constant S_{6666} is required to account for the in-plane shear nonlinearity. The value of S_{6666} can be determined by a curve fit to various off-axis tension test data (Hahn and Tsai 1973). Differentiating (5), we have

$$\Delta\left\{\begin{array}{c}\varepsilon_1\\ \varepsilon_2\\ \gamma_{12}\end{array}\right\} = \left[\begin{array}{ccc}\dfrac{1}{E_{11}} & -\dfrac{\nu_{21}}{E_{22}} & 0\\ -\dfrac{\nu_{12}}{E_{11}} & \dfrac{1}{E_{22}} & 0\\ 0 & 0 & \dfrac{1}{G_{12}}\end{array}\right]\Delta\left\{\begin{array}{c}\sigma_1\\ \sigma_2\\ \tau_{12}\end{array}\right\} +$$

$$3S_{6666}\tau_{12}^2\Delta\left\{\begin{array}{c}0\\ 0\\ \tau_{12}\end{array}\right\}. \tag{6}$$

Inverting the above equation, we obtain the nonlinear incremental constitutive matrix for the lamina

$$\mathbf{Q}_1' = \left[\begin{array}{ccc}\dfrac{E_{11}}{1-\nu_{12}\nu_{21}} & \dfrac{\nu_{12}E_{22}}{1-\nu_{12}\nu_{21}} & 0\\ \dfrac{\nu_{21}E_{11}}{1-\nu_{12}\nu_{21}} & \dfrac{E_{22}}{1-\nu_{12}\nu_{21}} & 0\\ 0 & 0 & \dfrac{1}{1/G_{12}+3S_{6666}\tau_{12}^2}\end{array}\right]. \tag{7}$$

3 Constitutive matrix for composite shell section

The elements used in finite-element analyses are eight-node isoparametric shell elements with six degrees of freedom per node (three displacements and three rotations). The formulation of the shell allows transverse shear deformation (Irons 1975; Hibbitt *et al.* 1993) and these shear flexible shells can be used for both thick and thin shell analysis (Hibbitt *et al.* 1993).

During a finite element analysis, the constitutive matrix of composite materials at the integration points of shell elements must be calculated before the stiffness matrices are assembled from the element level to the structural level. For fiber-composite laminate materials, the incremental constitutive equations of a lamina in the element coordinates (x, y, z) can be written as

$$\Delta\sigma = \mathbf{Q}_1\Delta\varepsilon, \tag{8}$$

$$\Delta\tau_t = \mathbf{Q}_2\Delta\gamma_t, \tag{9}$$

$$\mathbf{Q}_1 = \mathbf{T}_1^T\mathbf{Q}_1'\mathbf{T}_1, \tag{10}$$

$$\mathbf{Q}_2 = \mathbf{T}_2^T\mathbf{Q}_2'\mathbf{T}_2, \tag{11}$$

$$\mathbf{T}_1 = \left[\begin{array}{ccc}\cos^2\phi & \sin^2\phi & \sin\phi\cos\phi\\ \sin^2\phi & \cos^2\phi & -\sin\phi\cos\phi\\ -2\sin\phi\cos\phi & 2\sin\phi\cos\phi & \cos^2\phi-\sin^2\phi\end{array}\right], \tag{12}$$

$$\mathbf{T}_2 = \left[\begin{array}{cc}\cos\phi & \sin\phi\\ -\sin\phi & \cos\phi\end{array}\right], \tag{13}$$

where $\Delta\sigma = \Delta\{\sigma_x,\sigma_y,\tau_{xy}\}^T, \Delta\tau_t = \Delta\{\tau_{xz},\tau_{yz}\}^T, \Delta\varepsilon = \Delta\{\varepsilon_x,\varepsilon_y,\gamma_{xy}\}^T, \Delta\gamma_t = \Delta\{\gamma_{xz},\gamma_{yz}\}^T$, and ϕ is measured counterclockwise from the element local x-axis to the material 1-axis.

Assume that $\Delta\varepsilon_0 = \Delta\{\varepsilon_{x0},\varepsilon_{y0},\gamma_{xy0}\}^T$ are the incremental in-plane strains at the mid-surface of the section and $\Delta\kappa = \Delta\{\kappa_x,\kappa_y,\kappa_{xy}\}^T$ the incremental curvatures. The incremental in-plane strains at a distance z from the mid-surface of the shell section become

$$\Delta\varepsilon = \Delta\varepsilon_0 + z\Delta\kappa, \tag{14}$$

Let h be the total thickness of the shell section, the incremental stress resultants, $\Delta\mathbf{n} = \Delta\{n_x,n_y,n_{xy}\}^T$, $\Delta\mathbf{m} = \Delta\{m_x,m_y,m_{xy}\}^T$ and $\Delta\mathbf{v} = \Delta\{v_x,v_y\}$, can be defined as

$$\left\{\begin{array}{c}\Delta\mathbf{n}\\ \Delta\mathbf{m}\\ \Delta\mathbf{v}\end{array}\right\} = \int_{-h/2}^{h/2}\left\{\begin{array}{c}\Delta\sigma\\ z\Delta\sigma\\ \Delta\tau_t\end{array}\right\}dz =$$

$$\int_{-h/2}^{h/2}\left[\begin{array}{ccc}\mathbf{Q}_1 & z\mathbf{Q}_1 & \mathbf{D}\\ z\mathbf{Q}_1 & z^2\mathbf{Q}_1 & \mathbf{D}\\ \mathbf{D}^T & \mathbf{D}^T & \mathbf{Q}_2\end{array}\right]\left\{\begin{array}{c}\Delta\varepsilon_0\\ \Delta\kappa\\ \Delta\gamma_t\end{array}\right\}dz, \tag{15}$$

where $\mathbf{D}$ is a 3×2 matrix with all the coefficients equal to zero.

For the nonlinear material case, the $\mathbf{Q}_1'$ matrix in (10) is taken from (7) and the incremental stress resultants of (15) can be obtained by a numerical integration through the thickness of the composite shell section. For the linear material case, the $\mathbf{Q}_1'$ matrix used in (10) is taken from (3) and the incremental stress resultants of the shell section can be written as a summation of integrals over the k laminae in the following form:

$$\left\{\begin{array}{c}\Delta\mathbf{n}\\ \Delta\mathbf{m}\\ \Delta\mathbf{v}\end{array}\right\} =$$

$$\left(\sum_{j=1}^{k}\left[\begin{array}{ccc}(z_{jt}-z_{jb})\mathbf{Q}_1 & \frac{1}{2}(z_{jt}^2-z_{jb}^2)\mathbf{Q}_1 & \mathbf{D}\\ \frac{1}{2}(z_{jt}^2-z_{jb}^2)\mathbf{Q}_1 & \frac{1}{3}(z_{jt}^3-z_{jb}^3)\mathbf{Q}_1 & \mathbf{D}\\ \mathbf{D}^T & \mathbf{D}^T & (z_{jt}-z_{jb})\mathbf{Q}_2\end{array}\right]\right)\cdot$$

$$\left\{\begin{array}{c}\Delta\varepsilon_0\\ \Delta\kappa\\ \Delta\gamma_t\end{array}\right\}, \tag{16}$$

where z_{jt} and z_{jb} are distances from the mid-surface of the section to the top and the bottom of the j-th layer, respectively.

4 Nonlinear buckling analysis

In the ABAQUS finite element program, the nonlinear response of a structure is modelled by an updated Lagrangian formulation and a modified Riks nonlinear incremental algorithm (Riks 1979) can be used to construct the equilibrium solution path. To model bifurcation from the prebuckling path to the postbuckling path, geometric imperfections of composite shells are introduced by superimposing a small fraction of the lowest eigenmode, determined by a linearized buckling analysis, to the original nodal coordinates of the shell as

$$\mathbf{I} = \mathbf{O} + \beta \mathbf{h} \boldsymbol{\psi}, \tag{17}$$

where $\mathbf{I}$ is the resulting imperfect nodal coordinate of the shell, $\mathbf{O}$ is the original nodal coordinate of the shell, $\boldsymbol{\psi}$ is the normalized lowest eigenmode, and β is a scaling coefficient (say 0.001).

5 Sequential linear programming

Let $\mathbf{x} = \{x_1, x_2, \ldots, x_n\}^T$ be a vector of design variables. Generally, an optimization problem may be defined as follows:

$$\text{minimize}: f(\mathbf{x}), \tag{18a}$$

$$\text{subject to}: g_i(\mathbf{x}) \leq 0, \quad i = 1, \ldots, r, \tag{18b}$$

$$h_j(\mathbf{x}) = 0, \quad j = r+1, \ldots, m, \tag{18c}$$

$$p_k \leq x_k \leq q_k, \quad k = 1, \ldots, n, \tag{18d}$$

where $f(\mathbf{x})$ is an objective function, $g_i(\mathbf{x})$ are inequality constraints, and $h_j(\mathbf{x})$ are equalitiy constraints. If an optimization problem requires maximization, we simply minimize $-f(\mathbf{x})$.

The original optimization problem may be approximated by expanding the objective functions and constraints in Taylor series at a feasible solution point $\mathbf{x}_0 = \{x_{01}, x_{02}, \ldots, x_{0n}\}^T$ and ignoring terms of order higher than the linear ones. With this approximation, the optimization problem becomes

$$\text{minimize}: f(\mathbf{x}) \approx f(\mathbf{x}_0) + \nabla f(\mathbf{x}_0)^T \delta\mathbf{x}, \tag{19a}$$

$$\text{subject to}: g_i(\mathbf{x}) \approx g_i(\mathbf{x}_0) + \nabla g_i(\mathbf{x}_0)^T \delta\mathbf{x} \leq 0, \tag{19b}$$

$$h_j(\mathbf{x}) \approx h_j(\mathbf{x}_0) + \nabla h_j(\mathbf{x}_0)^T \delta\mathbf{x} = 0, \tag{19c}$$

$$p_k \leq x_k \leq q_k, \tag{19d}$$

where $\delta\mathbf{x} = \{x_1 - x_{01}, x_2 - x_{02}, \ldots, x_n - x_{0n}\}^T$. A solution for the above equations may be easily obtained by the Simplex method (Kolman and Beck 1980). After obtaining an initial approximate solution for (19a)-(19d), say $\mathbf{x}_1$, we can linearize the original problem, (18a)-(18d), at $\mathbf{x}_1$ and solve the new linear programming problem. The process is repeated until a convergent solution is obtained. This method leading to the optimal solution is usually termed the sequential linear programming technique (Zienkiewicz and Champbell 1973; Vanderplaats 1984).

Although the procedure for the sequential linear programming is simple, the optimum solution for the approximated linear problem may violate the constraint conditions of the original optimization problem. In addition, if the true optimum solution of the nonlinear problem appears between two constraint intersections, a straightforward successive linearization may lead to an oscillation of the solution between the widely separated values. Difficulties in dealing with such problems may be avoided by imposing a "move limit" (Zienkiewicz and Champbell 1973; Vanderplaats 1984) on the linear approximation, which is a set of box-like admissible constraints placed on the range of $\delta\mathbf{x}$. In general, the choice of a suitable move limit depends on experience and also on the results of previous steps. Once a proper move limit is chosen at the beginning of the sequential linear programming procedure, this move limit should gradually approach zero as the iterative process continues (Zienkiewicz and Champbell 1973; Vanderplaats 1984; Esping 1984).

The algorithm of the sequential linear programming with selected move limits may be summarized as follows: (1) linearize the nonlinear objective function and associated constraints with respect to an initial guess $\mathbf{x}_0$; (2) impose move limits in the form of $-\mathbf{a} \leq (\mathbf{x} - \mathbf{x}_0) \leq \mathbf{b}$, where $\mathbf{a}$ and $\mathbf{b}$ are properly chosen lower and upper bounds; (3) solve the approximate linear programming problem to obtain an optimum solution $\mathbf{x}_1$; (4) repeat the process by redefining $\mathbf{x}_1$ with $\mathbf{x}_0$ until either the subsequent solutions do not change significantly (i.e. true convergence) or the move limit approaches zero (i.e. forced convergence). If the solution obtained is due to forced convergence, the procedures from (1) to (4) should be repeated with another initial guess.

6 Numerical examples

6.1 Buckling optimization of composite shell with one design variable

In this section, a simply supported fiber-composite laminate cylindrical shell (Fig. 2) with laminate layup $[\pm\theta/90_2/0]_S$ under external hydrostatic compression p is investigated. The ends of the shell are closed and the uniform pressure loads applied at two end surfaces are transferred into equivalent concentrated ring loads applied at two circular edges. The shell is composed of graphite/epoxy and typical in-plane shear stress-strain curves are shown in Fig. 3. The objective of this study is to determine the optimal fiber angle θ to maximize the buckling load p_{cr} of the shell and to compare the result of the optimization using a nonlinear shear formulation with that using a linear shear formulation.

Based on the sequential linear programming, in each iteration the current linearized optimization problem becomes

$$\text{maximize}: p_{\mathrm{cr}}(\theta) \approx p_{\mathrm{cr}}(\theta_0) + (\theta - \theta_0) \frac{\partial p_{\mathrm{cr}}}{\partial \theta} \Big|_{\theta=\theta_0}, \tag{20a}$$

$$\text{subject to}: 0^\circ \leq \theta \leq 90^\circ, \tag{20b}$$

$$-r \times q \times 0.5^S \leq (\theta - \theta_0) \leq r \times q \times 0.5^S, \tag{20c}$$

where θ_0 is a solution in the current iteration. The symbols r and q are the size and the reduction rate of the move limit. In this study, the values of r and q are selected to be 10° and $0.9^{(N-1)}$, where N is the current iteration number. To control the oscillation of the solution, a parameter 0.5^S is introduced in the move limit (Hu and Wang 1992), where s is the number of sign changes for the derivative $\partial p_{\mathrm{cr}}/\partial\theta$ that has taken place before the current iteration. The derivative $\partial p_{\mathrm{cr}}/\partial\theta$ may be approximated by using a forward finite-difference method as follows:

$$\frac{\partial p_{\mathrm{cr}}}{\partial \theta} \approx \left[\frac{p_{\mathrm{cr}}(\theta_0 + \Delta\theta) - p_{\mathrm{cr}}(\theta_o)}{\Delta\theta}\right], \tag{21}$$

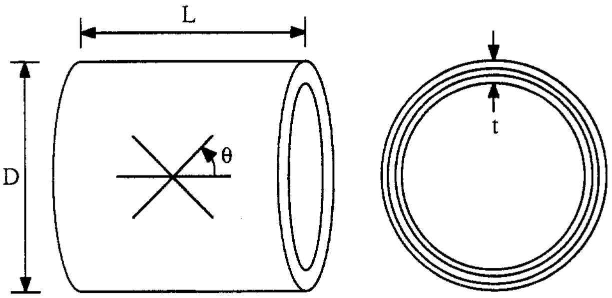

Laminate layup:
$[\pm\theta/90_2/0]_s$

Composite shell geometry:
L = 20.32 cm
D = 20.32 cm
t = 1.27 cm

Ply constitutive properties:
E_{11} = 138 GPa
E_{22} = 14.5 GPa
$G_{12} = G_{13}$ = 5.86 GPa
G_{23} = 3.52 GPa
ν_{12} = 0.21
S_{6666} = 7.32 $(GPa)^{-3}$

Fig. 2. Fiber-composite laminate cylindrical shell

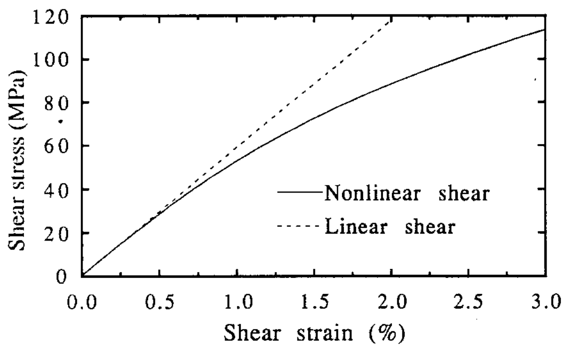

Fig. 3. In-plane shear stress-strain curves for graphite/epoxy composite lamina

Hence, two buckling analyses are required to compute $p_{cr}(\theta_0)$ and $p_{cr}(\theta_0+\Delta\theta)$ in each iteration. The value of $\Delta\theta$ is selected to be 1° in most iterations.

Important numerical results obtained in the optimization study are given in Fig. 4, which shows the fiber orientation θ and the associated critical buckling pressure p_{cr} determined in each iteration. The initial values of θ are selected to be 90° for both analyses using the linear and nonlinear shear formulations. For the solution based on the nonlinear shear formulation, after eleven iterations the optimal value of θ converges to 60.3° and the optimal critical buckling pressure converges to 175 MPa (true convergence). For the solution based on the linear shear formulation, after twelve iterations the optimal value of θ converges to 60.8° and the optimal critical buckling pressure converges to 176 MPa (true convergence).

Figure 5 shows the load-end displacement curves for the composite shells associated with the first iteration (initial guess) and the final iteration (optimal solution). It is clear that as the solution converges from the initial guess to the optimal solution not only the critical buckling pressure of the shell is increased but also the postbuckling strength of the shell is greatly improved. Under the initial guess condition, all fibers are oriented in 0° and 90° directions. The shear stresses of the shell are primarily resisted by resin, the main

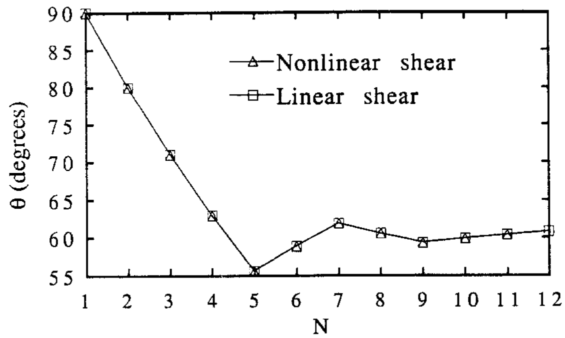

(a) Number of iterations N vs. fiber angle θ

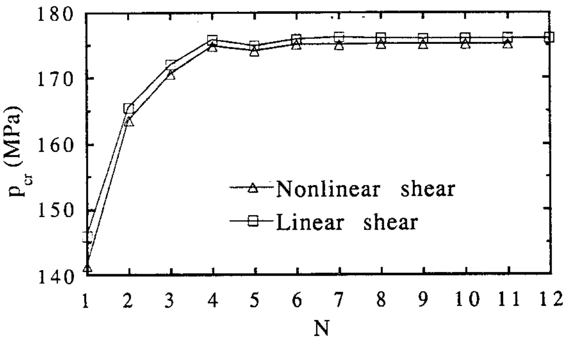

(b) Number of iterations N vs. critical pressure p_{cr}

Fig. 4. Buckling optimization of the simply supported $[\pm\theta/90_2/0]_S$ composite shell under hydrostatic compression, (a) number of iterations N vs. fiber angle θ, and (b) number of iterations N vs. critical pressure p_{cr}

subject causing the nonlinear shear. Hence, it is not surprising to see that there is a significant reduction on the critical pressure and the postbuckling strength of the composite shell using the nonlinear shear formulation. Under the optimal solution condition, the fibers are oriented in 0°, 60°, -60° and 90° directions. The shear stresses of the shell are resisted not only by resin but also by fibers. Consequently, the nonlinear shear effect is not expected to be significant and the buckling and the postbuckling behaviour of the composite shell using the nonlinear shear formulation are very similar to those of the shell using the linear shear formulation.

6.2 Buckling optimization of the composite shell with two design variables

In this section, the composite laminate shell with the same geometry, end condition and loading condition as that in the previous section but with unsymmetric laminate layup $[\pm\phi/90_2/0_2/90_2/\mp\theta]$ is investigated. The objectives of this study are to find the optimal fiber orientations ϕ and θ to maximize the critical buckling pressure of the composite shell, and to examine the influence of the nonlinear shear and the unsymmetric laminate layup on the results of optimization.

Based on the sequential linear programming, in each iteration the current linearized optimization problem becomes

maximize: $p_{cr}(\phi,\theta) \approx p_{cr}(\phi_0,\theta_0)+$

$$(\phi-\phi_0)\frac{\partial p_{cr}}{\partial\phi}\,|_{\phi=\phi_0,\theta=\theta_0}+(\theta-\theta_0)\frac{\partial p_{cr}}{\partial\theta}\,|_{\phi=\phi_0,\theta=\theta_0}\,, \quad (22a)$$

subject to: $0^\circ \leq \phi \leq 90^\circ$, (22b)

$$0^\circ \le \theta \le 90^\circ, \qquad (22c)$$

$$-r_1 \times q_1 \times 0.5^{S_1} \le (\phi - \phi_0) \le r_1 \times q_1 \times 0.5^{S_1}, \qquad (22d)$$

$$-r_2 \times q_2 \times 0.5^{S_2} \le (\theta - \theta_0) \le r_2 \times q_2 \times 0.5^{S_2}, \qquad (22e)$$

where ϕ_0 and θ_0 are the solutions in the current iteration. The values of r_1 and r_2 are selected to be 10°. The values of q_1 and q_2 are selected to be $0.9^{(N-1)}$, where N is a current iteration number. The s_1 and s_2 are the numbers of sign changes for the derivatives $\partial p_{\mathrm{cr}}/\partial\phi$ and $\partial p_{\mathrm{cr}}/\partial\theta$. These derivatives may be approximated with the following finite-difference forms:

$$\frac{\partial p_{\mathrm{cr}}}{\partial \phi} \approx \frac{[p_{\mathrm{cr}}(\phi_0 + \Delta\phi, \theta_0) - p_{\mathrm{cr}}(\phi_0, \theta_0)]}{\Delta\phi}, \qquad (23a)$$

$$\frac{\partial p_{\mathrm{cr}}}{\partial \theta} \approx \frac{[p_{\mathrm{cr}}(\phi_0, \theta_0 + \Delta\theta) - p_{\mathrm{cr}}(\phi_0, \theta_0)]}{\Delta\theta}. \qquad (23b)$$

Hence, three buckling analyses are required to compute $p_{\mathrm{cr}}(\phi_0, \theta_0), p_{\mathrm{cr}}(\phi_0 + \Delta\phi, \theta_0)$ and $p_{\mathrm{cr}}(\phi_0, \theta_0 + \Delta\theta)$ in each iteration. The values of $\Delta\phi$ and $\Delta\theta$ are selected to be 1° in most iterations.

Important numerical results obtained in the optimization study are given in Fig. 6, which shows the fiber conditions ϕ and θ, and the associated critical buckling pressure p_{cr} determined in each iteration. The initial values of ϕ and θ are selected to be 90° for both solutions using the linear and nonlinear shear formulations. For the solution based on the nonlinear shear formulation, after thirteen iterations the optimal values of ϕ and θ converge to 90° and 53.7°, respectively, and the optimal critical buckling pressure converges to 187 MPa (true convergence). For the solution based on the linear shear formulation, after twelve iterations the optimal values of ϕ and θ converge to 90° and 53.9°, respectively, and the optimal critical buckling pressure converges to 188 MPa (true convergence).

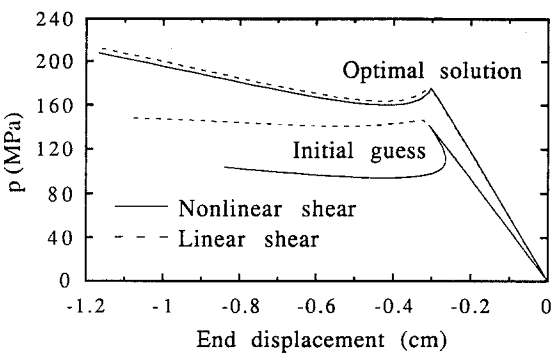

Fig. 5. Load-end displacement curves for the simply supported $[\pm\theta/90_2/0]_S$ composite shell under hydrostatic compression

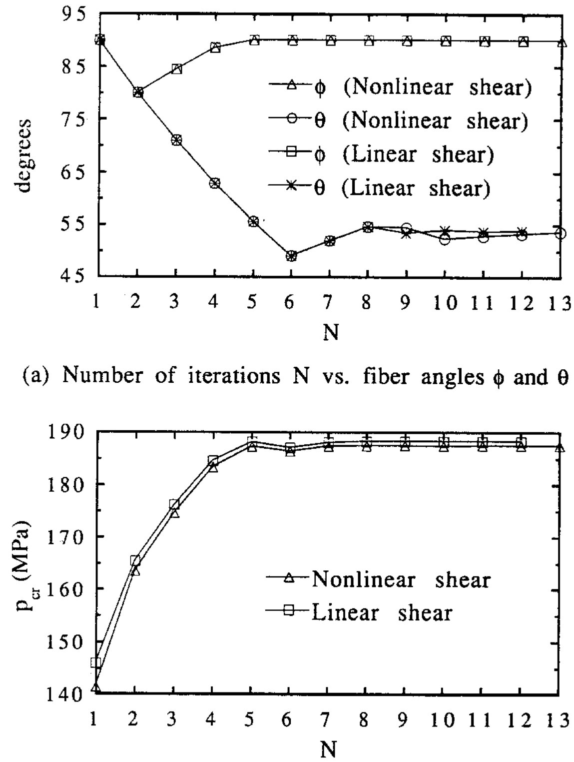

(a) Number of iterations N vs. fiber angles ϕ and θ

(b) Number of iterations N vs. critical pressure p_{cr}

Fig. 6. Buckling optimization of the simply supported $[\pm\phi/90_2/0_2/90_2/\mp\theta]$ composite shell under hydrostatic compression, (a) number of iterations N vs. fiber angles ϕ and θ, and (b) number of iterations N vs. critical pressure p_{cr}

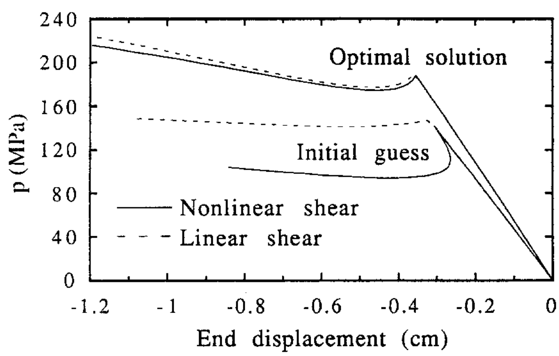

Fig. 7. Load-end displacement curves for simply supported $[\pm\phi/90_2/0_2/90_2/\mp\theta]$ composite shell under hydrostatic compression

Figure 7 shows the load-end displacement curves for the composite shells associated with the first iteration (initial guess) and the final iteration (optimal solution). Again, as the solution converges from the initial guess to the optimal solution not only the critical buckling pressure of the shell is increased but also the postbuckling strength of the shell is greatly improved. Under the initial guess condition, there is a significant reduction on the critical buckling pressure and the postbuckling strength of the composite shell using the nonlinear shear formulation. However, under the optimal solution condition, the buckling and the postbuckling behaviours of the composite shell using the nonlinear shear formulation are very similar to those of the shell using a linear shear formulation.

Figure 8 shows the load-end displacement curves under optimal fiber angle conditions for the composite shells with $[\pm\theta/90_2/0]_S$ and $[\pm\theta/90_2/0_2/90_2/\mp\theta]$ laminate layups. It can be seen that under optimal fiber angle conditions (no matter which shear formulation was used) the buckling and the postbuckling strengths of the composite shell with the unsymmetric laminate layup are significantly higher than those of the shell with the symmetric laminate layup. In the design of composite structures, unsymmetric composite laminates are seldom used because of the bending-extensional coupling effect. However, this example shows that it is beneficial to adopt an unsymmetric laminate layup (having more design degrees of freedom) to increase the buckling and the postbuckling strengths of the composite shell.

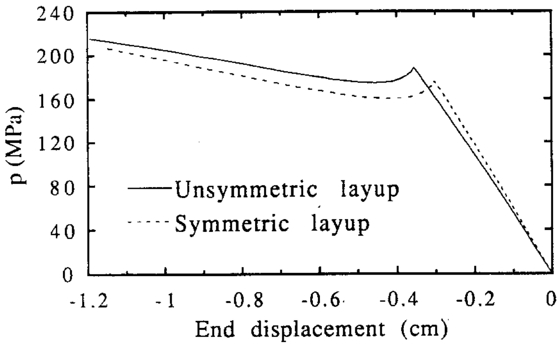

(a) with nonlinear shear formulation

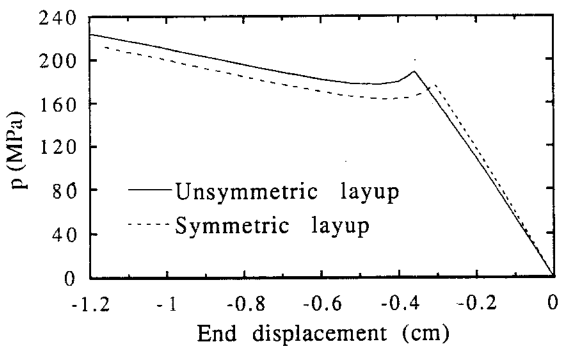

(b) with linear shear formulation

Fig. 8. Load-end displacement curves under optimal fiber angle conditions for simply supported composite shells under hydrostatic compression with symmetric layup $[\pm\theta/90_2/0]_S$ and with unsymmetric layup $[\pm\phi/90_2/0_2/90_2/\mp\theta]$

7 Conclusions

From the optimization results obtained in this study, the following conclusions can be drawn.

1. For the optimization of simply supported composite shells subjected to external hydrostatic compression with $[\pm\theta/90_2/0]_S$ and $[\pm\phi/90_2/0_2/90_2/\mp\theta]$ laminate layups, the optimal fiber angles θ and ϕ obtained by using the nonlinear in-plane shear formulation are very close to those obtained by using the linear in-plane shear formulation.
2. For simply supported composite shells with $[\pm\theta/90_2/0]_S$ and $[\pm\phi/90_2/0_2/90_2/\mp\theta]$ laminate layups, under initial guess conditions, the buckling and postbuckling strengths of the composite shell using the nonlinear in-plane shear formulation may be significantly lower than those of the shell using the linear in-plane shear formulation. This is because under initial guess conditions (with $\phi = \theta = 90^\circ$),all the fibers orient in 0° and 90°, and the composite shell is weak in resisting in-plane shear. Therefore, the nonlinear shear effect is significant. However, under optimal fiber angle conditions the buckling and the postbuckling behaviour of the composite shell using the nonlinear shear formulation are very similar to those of the shell using the linear shear formulation. This is because under optimal fiber angle conditions, there are some fibers oriented between 0° and 90°, and the composite shell is strong in resisting in-plane shear. Hence, the nonlinear shear effect is not significant.
3. Under optimal fiber angle conditions (no matter which shear formulation was used) the buckling and postbuckling strengths of the composite shell with the unsymmetric laminate layup $[\pm\phi/90_2/0_2/90_2/\mp\theta]$ are significantly higher than those of the shells with the symmetric laminate layup $[\pm\theta/90_2/0]_S$.

Received Feb. 23, 1993
Revised manuscript received April 6, 1994

References

Esping, B.J.D. 1984: Minimum weight design of membrane structures. *Computers and Structures* **19**, 707-716

Hahn, H.T.; Tsai, S.W. 1973: Nonlinear elastic behavior of unidirectional composite laminae. *J. Composite Materials* **7**, 102-118

Hashin, Z.; Bagchi, D.; Rosen, B.W. 1974: Non-linear behavior of fiber composite laminates. *NASA CR-2313*

Hibbitt, Karlsson and Sorensen, Inc. 1993: *ABAQUS theory manual and user manual, Version 5.2.* Providence, Rhode Island

Hu, H.-T.; Wang, S.S. 1992: Optimization for buckling resistance of fiber-composite laminate shells with and without cutouts. *Composite Structures* **22**, 3-13

Irons, B.M. 1976: The semi-loof shell element. In: Ashwell, D.G.; Gallagher, R.H. (eds.) *Finite elements for thin shells and curved members,* pp. 197-222. New York: Wiley

Kolman, B.; Beck, R.E. 1980: *Elementary linear programming with applications,* pp. 59-142. Orlando: Academic Press

Riks, E. 1979: An incremental approach to the solution of snapping and buckling problems. *Int. J. Solids & Struct.* **15**, 529-551

Sun, G.; Hansen, J.S. 1988: Optimal design of laminate-composite circular-cylindrical shells subjected to combined loads. *J. Appl. Mech.* **55**, 136-142.

Vanderplaats, G.N. 1984: *Numerical optimization techniques for engineering design with applications,* pp. 155-157. New York: McGraw-Hill.

Zienkiewicz, O.C.; Champbell, J.S. 1973: Shape optimization and sequential linear programming. In: Gallagher, R.H.; Zienkiewicz, O.C. (eds.) *Optimum structural design: theory and applications,* pp. 109-126. New York: Wiley